PHYSICS

Enantioselective fragmentation of an achiral molecule in a strong laser field

K. Fehre[1]*, S. Eckart[1], M. Kunitski[1], M. Pitzer[2], S. Zeller[1], C. Janke[1], D. Trabert[1], J. Rist[1], M. Weller[1], A. Hartung[1], L. Ph. H. Schmidt[1], T. Jahnke[1], R. Berger[3], R. Dörner[1], M. S. Schöffler[1]*

Chirality is omnipresent in living nature. On the single molecule level, the response of a chiral species to a chiral probe depends on their respective handedness. A prominent example is the difference in the interaction of a chiral molecule with left or right circularly polarized light. In the present study, we show by Coulomb explosion imaging that circularly polarized light can also induce a chiral fragmentation of a planar and thus achiral molecule. The observed enantiomer strongly depends on the orientation of the molecule with respect to the light propagation direction and the helicity of the ionizing light. This finding might trigger new approaches to improve laser-driven enantioselective chemical synthesis.

INTRODUCTION

The concept of chirality, the property of an object to be distinguishable from its mirror image, can be found in nature in various regimes: Our hands, for example, snail shells, and even small molecules can occur in a distinct handedness. Whereas molecular enantiomers, i.e., the molecule and its mirror image, have the same binding energies when neglecting a minuscule contribution of the parity-violating weak force (*1*–*3*), their handedness profoundly affects, in some cases, their interaction with other chiral objects. This property is particularly important as such objects can, for example, be receptors in living cells. For this reason, in chemistry and pharmaceutics, methods for enantioselective synthesis or at least enantioselective purification are crucial. Circularly polarized light could serve as an enantioselective agent and potentially replace expensive or environmentally harmful catalysts (*4*, *5*). Since the first report on enantioselective photolysis in 1929 (*6*), theoretical proposals have been made to use coherent control schemes to this end (*7*–*9*). Until no approach developed so far has achieved high efficiency. Moreover, for the existing techniques, a microscopic understanding is lacking, for example, regarding the influence of structural dynamics (*10*, *11*).

A possible way to investigate in detail the influence of light on molecular chirality is to start from an initially achiral species and search for a chiral signal and enantiomeric excess after irradiation. We pursue this route using formic acid (HCOOH), a molecule in which the carbon atom is sp^2 hybridized and its three bonding partners are in a planar arrangement in the electronic ground state (Fig. 1, see center of the sphere). It is known that the n→π* excitation, with a vertical transition energy of about 5.9 eV, leads to pyramidalization, creating a chiral equilibrium configuration (*12*–*14*). In a simplified picture, an electron from the nonbonding orbital at the carbonyl oxygen atom is transferred upon excitation to the antibonding π* orbital of the carbonyl group (*13*). In the equilibrium structure of this electronically excited state, the carbonyl oxygen (referred to as O_1 hereafter) is moved out of plane relative to the nearly coplanar other four atoms. If we use the three heavy atoms as reference instead, which will be favorable for the following discussion, the hydrogen at the carbonyl group (H_1) is bent on average by 32° out of the plane (*14*), which is spanned by the carbonyl oxygen (O_1), the hydroxyl oxygen (O_2), and the C atom. This displacement of H_1 is accompanied by a torsional motion of the acidic hydrogen H_2 in the opposite direction.

Although the π* exited state is not the only possible step in the electronic excitation and subsequent ionization process, the structure of this state shows close agreement with those presented in Fig. 2 (A and C). The observed enantiomer can be selected with high fidelity by the direction from which the light impinges onto the molecule. In our experiment, we achieve enantioselective pyramidalization and imaging within the same strong, circularly polarized femtosecond laser pulse: The pulse (after inducing the structural changes) peels off several electrons of the molecule and breaks it up into five singly charged ions. These five ions are driven apart by Coulomb repulsion, and we image the handedness by measuring the emission directions of the ions in coincidence using COLTRIMS (cold target recoil ion momentum spectroscopy) (see Materials and Methods) (*15*, *16*). From the correlation angles between the fragments, the otherwise indistinguishable two O^+ and two H^+ can be assigned with an estimated fidelity of 81% to the O_1, O_2 and H_1, H_2 atoms in the molecule (see Materials and Methods; for the estimation of the assignment error, please refer to the Supplementary Materials). With this method, the molecular orientation in the laboratory frame can also be deduced from the measurement. During the analysis, the fragments generated in the Coulomb explosion are sorted by their orientation, allowing us to infer the light propagation direction in the molecular frame for each event. Accordingly, there is no need to actively align the molecules in space and a randomly oriented gas-phase sample can be used in our experiment.

The handedness of the fragmenting molecule can be characterized by a normalized triple product $\cos(\alpha) = (\vec{k}_{O2} \times \vec{k}_{O1}) \bullet \vec{k}_{H1} / (|\vec{k}_{O2} \times \vec{k}_{O1}| \bullet |\vec{k}_{H1}|)$ (*17*, *18*) containing the linear momentum vectors $\vec{k}_{H1}$, $\vec{k}_{O1}$, $\vec{k}_{O2}$ of the three ions bound to the carbon center. It provides the emission angle of the H_1 ion with respect to the normal of the plane defined by the momenta of the two oxygen atoms. The triple product is zero for a planar breakup, and positive values indicate that the molecule breaks up as the *R* enantiomer and negative values indicate the breakup as the *S* enantiomer (see the Supplementary Materials for a brief discussion of the convention used here). $\cos(\alpha)$ varies from 0 to ±1, where the maximum absolute values correspond to the linear momentum vector of H_1 being normal to the plane spanned by the linear momenta of O_2 and O_1. The sign of $\cos(\alpha)$ is positive when the linear momenta of O_2, O_1, and H_1 span in the given sequence a right-handed coordinate frame and negative for a left-handed coordinate frame.

[1]Institut für Kernphysik Goethe-Universität Frankfurt, Max-von-Laue-Str. 1, 60438 Frankfurt, Germany. [2]Chemical Physics Department, Weizmann Institute of Science, P.O. Box 26, 76100 Rehovot, Israel. [3]Fachbereich Chemie, Philipps-Universität Marburg, Hans-Meerwein-Straße 4, 35032 Marburg, Germany.
*Corresponding author. Email: fehre@atom.uni-frankfurt.de (K.F.); schoeffler@atom.uni-frankfurt.de (M.S.S.)

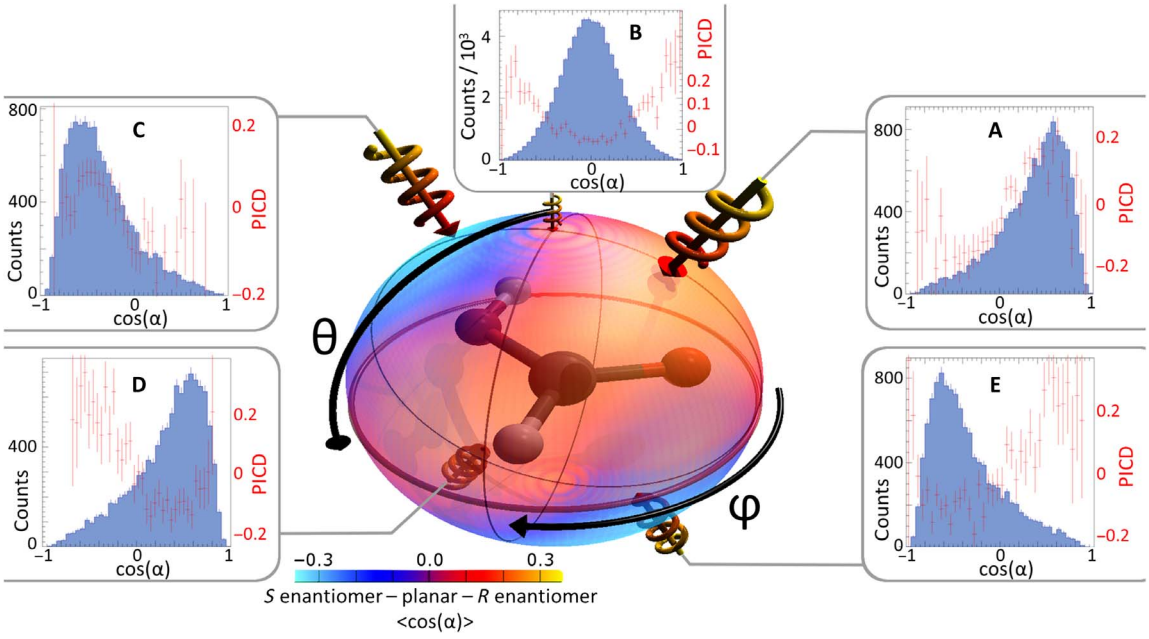

Fig. 1. Enantioselective fragmentation of formic acid. Center: Achiral formic acid in syn-conformation. The mean value of cos(α) is color-coded in the enveloping sphere for the corresponding propagation direction of the laser in the molecular system. The colored arrows and helices indicate the directions of incidence for LCP. (**A** to **E**) For selected directions, the surrounding panels show the distribution of cos(α) in blue and the photoion circular dichroism (PICD) as the normalized difference between distributions for right- and left-handed circularly polarized light (RCP and LCP) in red.

RESULTS AND DISCUSSION

The arrows in Fig. 1 connect the distributions of cos(α) (in blue) with the direction from which the light encounters the molecular system. For different directions of the light, large changes in the distribution of cos(α) can be observed (see Fig. 1, A to C). If one chooses a molecular orientation for which the light impinges from the opposite direction (for Fig. 1A, panel D and for Fig. 1C, panel E), in the molecular system, the direction of rotation of the electric field vector is inverted. Thus, the distribution differences seen in Fig. 1C and in Fig. 1A can be correlated with the influence of the helicity of the light. The mean value of cos(α) as a function of the direction from which the circularly polarized laser pulse hits the initially planar molecule is color-coded on the sphere surrounding the molecule. Planar molecules and simple racemic mixtures yield a mean value of zero. Thus, the prominent red and blue areas on this sphere give an indication of the induced enantiomeric excess.

The measured emission angles occurring after the Coulomb explosion suggest that for certain molecular orientations with respect to the polarization plane of the impinging light, the H_1 and H_2 atoms are bent out of the molecular plane. To visualize this out-of-plane bending, we show the full breakup structure for three characteristic cases in Fig. 2. These figures confirm that in the pyramidalized structure, the H_1 and H_2 atoms (the data for the latter are omitted in these figures) are bent out of the plane, which is in good agreement with the quantum chemically calculated equilibrium structure of the molecule in the n→π* excited state. Inspecting the four orientations that yield the maximum enantioselectivity of the excitation (Fig. 1), we find that the linear momenta of the protons point in the direction of the laser field. For the polar angle cos(θ) = 0.7, the molecular orientations with the highest enantiomeric excess coincide with the maximum count rate, suggesting an enhanced ionization probability for this chiral structure and molecular orientation. The highest overall count rates are achieved at the poles of the sphere (cos(θ) = −1, 1), i.e., for light impinging perpendicularly

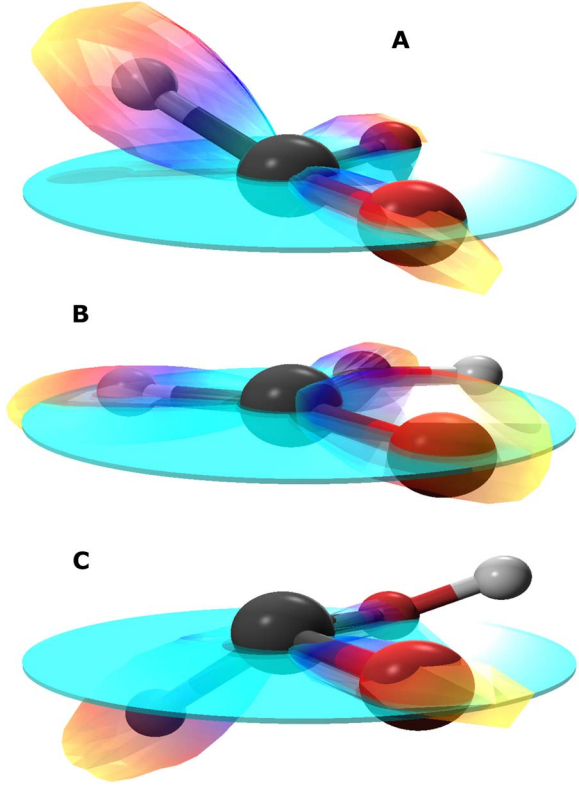

Fig. 2. Chiral and achiral structures of formic acid. The selected different molecular orientations with respect to the laser propagation direction are indicated in Fig. 1. The ball-and-stick model indicates the direction of the linear momentum vectors, and the transparent lobes represent the measured data; the distance from the C atom and color shows the count rate in the respective direction. The O–C=O plane is highlighted in turquoise. The letters connect the structures with the panels in Fig. 1. (**A**) *R* enantiomer. (**B**) Achiral structure. (**C**) *S* enantiomer.

onto the initially planar molecule, which is consistent with the naive picture of a tunneling ionization induced by the rotating electric field vector (*19*, *20*).

Last, both the relative orientation of the molecule with respect to the light propagation direction and the helicity of the light might influence the fragmentation. This helicity dependence is commonly characterized by the PICD, which is given as the normalized difference between the count rates $N_{LCP,RCP}$ for coincident detection of five singly charged atomic ions induced by left-handed circularly polarized (LCP) light (from the point of view of the source) and right-handed circularly polarized (RCP) light, respectively (details are in the Supplementary Materials) (*21*, *22*)

$$\mathrm{PICD} = \frac{N_{RCP} - N_{LCP}}{N_{LCP} + N_{RCP}}$$

The upper hemisphere (the top view onto the molecular plane) is chosen to be the case where, for the LCP light, the electric field vector sweeps the ligands in the sequence O_1-H-O_2, e.g., the light propagates toward the molecule from the *Si* face.

With this definition, we can inspect the PICD for any given impact direction of the light, i.e., for each point on the globe in Fig. 1. For one selected enantiomer [cos(α) > 0], Fig. 3A shows this PICD map. From the left (ϕ > 0) to the right (ϕ < 0) hemisphere (see Fig. 1 for the definition of angle ϕ), the PICD inverts. At most angles, its magnitude is between 0.1 and 0.2.

It is instructive to quantify the PICD as a function of cos(α) (Fig. 3, C to F). We find that the pattern of PICD changes and, even more notably, the overall PICD increases in magnitude with increasing cos(α). This is summarized in Fig. 3G, where the mean value of the magnitude of the PICD is associated with how strongly chirality is reflected for this conformer: cos(α) = 0 corresponds to a planar arrangement around the carbon atom. In particular, we would like to emphasize three points: First, the strength of the PICD depends on cos(α) and does not vanish even for very small absolute values of cos(α). Toward smaller absolute values of cos(α), the mean absolute PICD (Fig. 3G) gets smaller but does not seem to vanish if cos(α) goes to zero. This finite value is presumed to be due to different interaction of RCP and LCP with prochiral molecule fixed in space. Second, large changes become visible in the PICD pattern (Fig. 3, C to F), mostly positive and negative contributions going from the polar angle cos(θ) = 1 to cos(θ) = −1 or vice versa. Thus, the PICD [as well as the photoelectron circular dichroism (*23*–*26*)] is a probe for the molecular structure. Third, that an anisotropy of the PICD can be observed for a planar molecule is in correspondence with the observed anisotropy of conventional optical rotation for oriented achiral molecules with C_s point group symmetry (*27*).

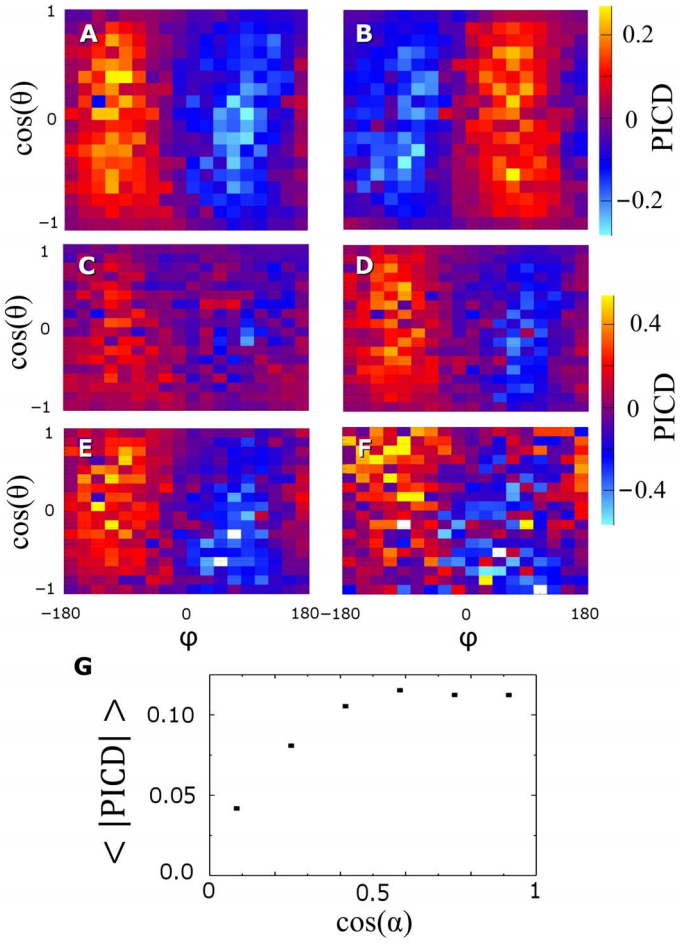

Fig. 3. Differential PICD of formic acid. (**A**) PICD for the *R* enantiomer. (**B**) PICD for the *S* enantiomer. The normalized difference was generated from the histogram for the (A) *R* enantiomer [with the *S* enantiomer in (B)] with LCP with the direction of the laser beam in the molecular system and those with RCP. (**C** to **F**) PICD with gating on cos(α). (C) 0 < |cos(α)| < 0.25. (D) 0.25 < |cos(α)| < 0.5. (E) 0.5 < |cos(α)| < 0.75. (F) 0.75 < |cos(α)| < 1. (**G**) Mean of the absolute value of the PICD versus cos (α) with $< |\mathrm{PICD}| > = \iint_{-1,-180}^{1,180} |\mathrm{PICD}(\cos(\theta), \varphi, \cos(\alpha))| d\cos(\theta) d\varphi$.

CONCLUSION

Our work shows that short, circularly polarized laser pulses can induce chirality enantioselectively for a prochiral molecule. This effect depends strongly on the relative spatial orientation of the molecule with respect to the light propagation direction as well as to the helicity of the light. Our observation can pave the way for future, purely light-driven control of stereochemistry starting from achiral precursors. To this end, the molecules can be prepared in a specific orientation, for example, with a

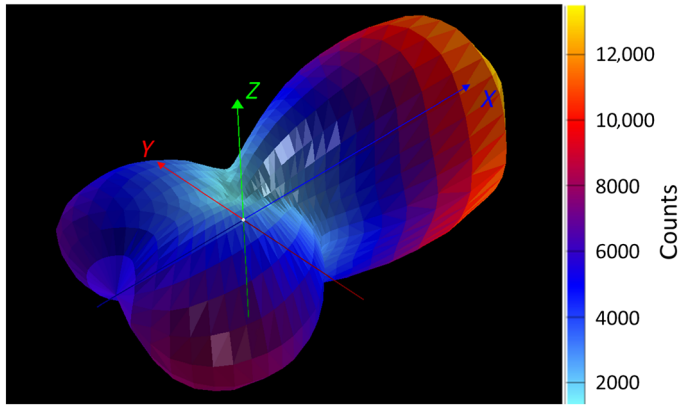

Fig. 4. Assignment of the fragments of the Coulomb explosion. The linear momenta of the H atoms in the molecular frame are plotted for the assignment of the fragments. The linear momentum of the C ion defines the *x* direction; together with the linear momentum of the O ions, it defines the *xy* plane. The angle in the coordinate system indicates the direction of the linear momentum vector, while the distance and the color scale indicate the number of counts along this direction.

preceding long-wavelength laser pulse (*28*); the result would be access to a laser-based enantiomer-specific manipulation of a chiral molecule. The use of femtosecond laser pulses also opens the door to time-resolved studies. Furthermore, it can be combined with other ultrafast probes of chirality such as photoelectron circular dichroism.

MATERIALS AND METHODS

Measuring five ions in coincidence requires a high detection efficiency. A COLTRIMS spectrometer was built (21-cm acceleration length and E = 119 V/cm electric field). The spectrometer was equipped with a position and time-sensitive detector [Hamamatsu microchannel plate (MCP); open area ratio (OAR)–specified 90% (*29*), combined with a second MCP for further amplification and followed by a hexagonal delay-line anode (*30*)] with an active diameter of 80 mm. The ions were accelerated to a kinetic energy of approximately 2.5 keV on their way to the detector. Therefore, no meshes are needed to be installed in front of the MCP, which is typically done for post-acceleration to increase the MCP's quantum efficiency. The main chamber was baked for 1 week at 360 K, resulting in a residual gas pressure without gas jet of 1×10^{-10} mbar. The ionization of the formic acid molecules was induced by focusing a short, intense, circularly polarized light (f = 60 mm, 40 fs, central wavelength of 800 nm, 1.3 W), generated by a Ti:sapphire regenerative amplifier (KMLabs Wyvern 500), resulting in a focal intensity of 1.3×10^{15} W/cm^2 onto the supersonic gas jet. Switching the helicity of the light with a motorized stage every 3 min ensured the same experimental conditions for the left and right circular polarization (LCP and RCP). The jet was produced by expanding formic acid with its vapor pressure at room temperature (approximately 44.6 mbar) through a nozzle (heated to reduce clustering, 340 K) of 30 μm diameter into vacuum.

With the COLTRIMS spectrometer, one can distinguish the fragments according to their mass-to-charge ratio similar to the usual time-of-flight spectrometer (TOF). Contrary to the latter, the arrival time combined with the impact position on the detector additionally allows the calculation of direction and magnitude of the ions' linear momenta. The five-particle breakup was identified by its photoion-photoion coincidence map, as explained elsewhere (*31*). For the assignment of O_1 and O_2 or H_1 and H_2 (that have the same mass), we made use of the molecular structure: All linear momentum vectors of the atoms were rotated in space such that the momentum of the carbon ion, which is identified by its TOF, points in the direction of the x axis (Fig. 4), and the linear momenta of the two oxygen ions define the xy plane. Subsequently, the hydrogen atoms were plotted. The proton whose momentum is pointing in the same direction as the carbon's momentum was assigned as H_1 and the other H atom as H_2. The O atom being on the same side of the xz plane as H_2 is the O_2 atom. Experiments on the partially deuterated formic acid-d (HCOOD) confirmed that proton migration does not occur before Coulomb explosion (*32*). The angle between the x axis and the H_1 momentum vector was required to be smaller than acos(0.4), and for the H_2 momentum vector, the angle was gated to be between acos(0.4) and acos(−0.8). From all completely detected five particle breakups, this method allows us to assign the fragments in 59% of the events. Because the enantiomers differ by the momentum component in the z direction, this selection does not affect the enantiomeric distribution. These safety margins ensure the correct assignment. By this type of assignment, one has access only to molecules that were in the ground state present as a syn-conformer (*14*). A comparison of the H atoms ejected in the direction of the C atom and those heading in the opposite direction suggests that this is the predominant configuration in the experiment. The size $N_{LCP,RCP}$ thus refers to the fivefold breakup, where all fragments could be assigned as described above.

SUPPLEMENTARY MATERIALS

Supplementary material for this article is available at http://advances.sciencemag.org/cgi/content/full/5/3/eaau7923/DC1

Notes to the *R/S* and *Re/Si* assignment

Dynamic chirality and the projection of the initial geometry to the final linear momenta by Coulomb explosion imaging

Estimation of the assignment error

Fig. S1. Simulation of the Coulomb explosion.

Fig. S2. The presentation of $\cos(\alpha)_{\text{initial-position}}$ as a function of $\cos(\alpha)$.

Fig. S3. Enantiomeric excess as a function of $\cos(\alpha)$.

References (*33*–*36*)

REFERENCES AND NOTES

1. M. Quack, J. Stohner, Influence of parity violating weak nuclear potentials on vibrational and rotational frequencies in chiral molecules. *Phys. Rev. Lett.* **84**, 3807–3810 (2000).
2. B. Darquié, C. Stoeffler, A. Shelkovnikov, C. Daussy, A. Amy-Klein, C. Chardonnet, S. Zrig, L. Guy, J. Crassous, P. Soulard, P. Asselin, T. R. Huet, P. Schwerdtfeger, R. Bast, T. Saue, Progress toward the first observation of parity violation in chiral molecules by high-resolution laser spectroscopy. *Chirality* **22**, 870–884 (2010).
3. M. Quack, How important is parity violation for molecular and biomolecular chirality? *Angew. Chem. Int. Ed. Engl.* **41**, 4618–4630 (2002).
4. H. Lorenz, A. Seidel-Morgenstern, Processes to separate enantiomers. *Angew. Chem. Int. Ed. Engl.* **53**, 1218–1250 (2014).
5. J. Martens, R. Bhushan, Purification of enantiomeric mixtures in enantioselective synthesis: Overlooked errors and scientific basis of separation in achiral environment. *Helv. Chim. Acta* **97**, 161–187 (2014).
6. W. Kuhn, E. Braun, Photochemische Erzeugung optisch aktiver Stoffe. *Naturwissenschaften* **17**, 227–228 (1929).
7. R. P. Cameron, S. M. Barnett, A. M. Yao, Discriminatory optical force for chiral molecules. *New J. Phys.* **16**, 013020 (2014).
8. D. Gerbasi, M. Shapiro, P. Brumer, Theory of "laser distillation" of enantiomers: Purification of a racemic mixture of randomly oriented dimethylallene in a collisional environment. *J. Chem. Phys.* **124**, 074315 (2006).
9. E. F. Thomas, N. E. Henriksen, Non-resonant dynamic stark control of vibrational motion with optimized laser pulses. *J. Chem. Phys.* **144**, 244307 (2016).
10. R. Neier, A two-catalyst photochemistry route to homochiral rings. *Science* **344**, 368–369 (2014).
11. A. Tröster, R. Alonso, A. Bauer, T. Bach, Enantioselective intermolecular [2 + 2] photocycloaddition reactions of 2(1*H*)-quinolones induced by visible light irradiation. *J. Am. Chem. Soc.* **138**, 7808–7811 (2016).
12. C. Fridh, Electronic excitation of formic acid. *J. Chem. Soc. Faraday Trans.* **74**, 190–193 (1978).
13. T. L. Ng, S. Bell, The π*←n transition of formic acid. *J. Mol. Spectrosc.* **50**, 166–181 (1974).
14. L. M. Beaty-Travis, D. C. Moule, E. C. Lim, R. H. Judge, A conformational study of the *S*1(n,π*) excited state of formic acid. *J. Chem. Phys.* **117**, 4831–4838 (2002).
15. R. Dörner, V. Mergel, O. Jagutzki, L. Spielberger, J. Ullrich, R. Moshammer, H. Schmidt-Böcking, Cold target recoil ion momentum spectroscopy: A 'momentum microscope' to view atomic collision dynamics. *Phys. Rep.* **330**, 95–192 (2000).
16. J. Ullrich, R. Moshammer, A. Dorn, R. Dörner, L. Ph. H. Schmidt, H. Schmidt-Böcking, Recoil-ion and electron momentum spectroscopy: Reaction-microscopes. *Rep. Prog. Phys.* **66**, 1463–1545 (2003).
17. M. Pitzer, K. Fehre, M. Kunitski, T. Jahnke, L. Schmidt, H. Schmidt-Böcking, R. Dörner, M. Schöffler, Coulomb explosion imaging as a tool to distinguish between stereoisomers. *J. Vis. Exp.* **126**, e56062 (2017).
18. M. Pitzer, M. Kunitski, A. S. Johnson, T. Jahnke, H. Sann, F. Sturm, L. Ph. H. Schmidt, H. Schmidt-Böcking, R. Dörner, J. Stohner, J. Kiedrowski, M. Reggelin, S. Marquardt, A. Schießer, R. Berger, M. S. Schöffler, Direct determination of absolute molecular stereochemistry in gas phase by Coulomb explosion imaging. *Science* **341**, 1096–1100 (2013).
19. L. Holmegaard, J. L. Hansen, L. Kalhøj, S. L. Kragh, H. Stapelfeldt, F. Filsinger, J. Küpper, G. Meijer, D. Dimitrovski, M. Abu-samha, C. P. J. Martiny, L. B. Madsen, Photoelectron

angular distributions from strong-field ionization of oriented molecules. *Nat. Phys.* **6**, 428–432 (2010).
20. S.-F. Zhao, C. Jin, A.-T. Le, T. F. Jiang, C. D. Lin, Determination of structure parameters in strong-field tunneling ionization theory of molecules. *Phys. Rev. A* **81**, 033423 (2010).
21. P. Horsch, G. Urbasch, K.-M. Weitzel, Analysis of chirality by femtosecond laser ionization mass spectrometry. *Chirality* **24**, 684–690 (2012).
22. U. Boesl von Grafenstein, A. Bornschlegl, Circular dichroism laser mass spectrometry: Differentiation of 3-methylcyclopentanone enantiomers. *Chemphyschem* **7**, 2085–2087 (2006).
23. G. Contini, N. Zema, S. Turchini, D. Catone, T. Prosperi, V. Carravetta, P. Bolognesi, L. Avaldi, V. Feyer, Vibrational state dependence of β and *D* asymmetry parameters: The case of the highest occupied molecular orbital photoelectron spectrum of methyl-oxirane. *J. Chem. Phys.* **127**, 124310 (2007).
24. S. Turchini, D. Catone, N. Zema, G. Contini, T. Prosperi, P. Decleva, M. Stener, F. Rondino, S. Piccirillo, K. C. Prince, M. Speranza, Conformational sensitivity in photoelectron circular dichroism of 3-methylcyclopentanone. *Chemphyschem* **14**, 1723–1732 (2013).
25. S. Turchini, D. Catone, G. Contini, N. Zema, S. Irrera, M. Stener, D. D. Tommaso, P. Decleva, T. Prosperi, Conformational effects in photoelectron circular dichroism of alaninol. *Chemphyschem* **10**, 1839–1846 (2009).
26. D. Di Tommaso, M. Stener, G. Fronzoni, P. Decleva, Conformational effects on circular dichroism in the photoelectron angular distribution. *Chemphyschem* **7**, 924–934 (2006).
27. H. Kimura, Theory of optical activity in nematic liquid crystals. *J. Phys. Soc. Jpn.* **30**, 1273–1279 (1971).
28. L. Christensen, J. H. Nielsen, C. S. Slater, A. Lauer, M. Brouard, H. Stapelfeldt, Using laser-induced Coulomb explosion of aligned chiral molecules to determine their absolute configuration. *Phys. Rev. A* **92**, 033411 (2015).
29. K. Fehre, D. Trojanowskaja, J. Gatzke, M. Kunitski, F. Trinter, S. Zeller, L. Ph. H. Schmidt, J. Stohner, R. Berger, A. Czasch, O. Jagutzki, T. Jahnke, R. Dörner, M. S. Schöffler, Absolute ion detection efficiencies of microchannel plates and funnel microchannel plates for multi-coincidence detection. *Rev. Sci. Instrum.* **89**, 045112 (2018).
30. O. Jagutzki, A. Cerezo, A. Czasch, R. Dorner, M. Hattas, M. Huang, V. Mergel, U. Spillmann, K. Ullmann-Pfleger, T. Weber, H. Schmidt-Bocking, G.D.W. Smith, Multiple hit readout of a microchannel plate detector with a three-layer delay-line anode. *IEEE Trans. Nucl. Sci.* **49**, 2477–2483 (2002).
31. M. Pitzer, G. Kastirke, M. Kunitski, T. Jahnke, T. Bauer, C. Goihl, F. Trinter, C. Schober, K. Henrichs, J. Becht, S. Zeller, H. Gassert, M. Waitz, A. Kuhlins, H. Sann, F. Sturm, F. Wiegandt, R. Wallauer, L. Ph. H. Schmidt, A. S. Johnson, M. Mazenauer, B. Spenger, S. Marquardt, S. Marquardt, H. Schmidt-Böcking, J. Stohner, R. Dörner, M. Schöffler, R. Berger, Absolute configuration from different multifragmentation pathways in light-induced Coulomb explosion imaging. *Chemphyschem* **17**, 2465–2472 (2016).
32. H. K. Gill, thesis, Experimental Atomic Physics at the Goethe-University Frankfurt (2015).
33. K. R. Hanson, Applications of the Sequence Rule. I. Naming the paired ligands g,g at a tetrahedral atom Xggij. II. Naming the two faces of a trigonal atom Yghi. *J. Am. Chem. Soc.* **88**, 2731–2742 (1966).
34. T. Kitamura, T. Nishide, H. Shiromaru, Y. Achiba, N. Kobayashi, Direct observation of "dynamic" chirality by Coulomb explosion imaging. *J. Chem. Phys.* **115**, 5–6 (2001).
35. A. M. Sayler, E. Eckner, J. McKenna, B. D. Esry, K. D. Carnes, I. Ben-Itzhak, G. G. Paulus, Nonunique and nonuniform mapping in few-body Coulomb-explosion imaging. *Phys. Rev. A* **97**, 033412 (2018).
36. T. Jahnke, L. Foucar, J. Titze, R. Wallauer, T. Osipov, E. P. Benis, A. Alnaser, O. Jagutzki, W. Arnold, S. K. Semenov, N. A. Cherepkov, L. Ph. H. Schmidt, A. Czasch, A. Staudte, M. Schöffler, C. L. Cocke, M. H. Prior, H. Schmidt-Böcking, R. Dörner, Vibrationally resolved *K*-shell photoionization of CO with circularly polarized light. *Phys. Rev. Lett.* **93**, 083002 (2004).

Acknowledgments: We thank H. Schmidt-Böcking, T. Baumert, and A. Senftleben for inspiring discussions. **Funding:** We acknowledge support from Deutsche Forschungsgemeinschaft via Sonderforschungsbereich 1319 (ELCH). K.F. and A.H. acknowledge support by the German National Merit Foundation. M.S.S. thanks the Adolf-Messer Foundation for financial support. **Author contributions:** K.F., S.E., M.K., M.P., S.Z., C.J., D.T., J.R., M.W., A.H., L.Ph.H.S., T.J., R.D., and M.S.S. contributed to the experiment. R.B. performed calculations. K.F., M.K., and M.P. performed classical molecular dynamics simulations. K.F., M.S.S., and R.D. did the data analysis. All authors contributed to the manuscript. **Competing interests:** The authors declare that they have no competing interests. **Data and materials availability:** All data needed to evaluate the conclusions in the paper are present in the paper and/or the Supplementary Materials. Additional data related to this paper may be requested from the authors. Correspondence and requests for materials should be addressed to K.F. (fehre@atom.uni-frankfurt.de), R.D. (doerner@atom.uni-frankfurt.de), or M.S.S. (schoeffler@atom.uni-frankfurt.de).

Submitted 16 July 2018
Accepted 24 January 2019
Published 8 March 2019
10.1126/sciadv.aau7923

Citation: K. Fehre, S. Eckart, M. Kunitski, M. Pitzer, S. Zeller, C. Janke, D. Trabert, J. Rist, M. Weller, A. Hartung, L. P. H. Schmidt, T. Jahnke, R. Berger, R. Dörner, M. S. Schöffler, Enantioselective fragmentation of an achiral molecule in a strong laser field. *Sci. Adv.* **5**, eaau7923 (2019).

Science Advances

Enantioselective fragmentation of an achiral molecule in a strong laser field

K. Fehre, S. Eckart, M. Kunitski, M. Pitzer, S. Zeller, C. Janke, D. Trabert, J. Rist, M. Weller, A. Hartung, L. Ph. H. Schmidt, T. Jahnke, R. Berger, R. Dörner and M. S. Schöffler

Sci Adv **5** (3), eaau7923.
DOI: 10.1126/sciadv.aau7923